Formation mechanism of thiophosphate anions in the liquid-phase synthesis of sulfide solid electrolytes using polar aprotic solvents

[1]Marcela Calpa, [2]Nataly Carolina Rosero-Navarro*, [2]Akira Miura, [3]Kota Terai, [3]Futoshi Utsuno, [2]Kiyoharu Tadanaga

1 Graduate School of Chemical Sciences and Engineering, Hokkaido University, Hokkaido 060-8628, Japan

2 Faculty of Engineering, Hokkaido University, Hokkaido 060-8628, Japan

3 Advanced Technology Research Laboratories, Idemitsu Kosan Co., Ltd., Chiba 299-0293, Japan

* Corresponding author

E-mail address: rosero@eng.hokudai.ac.jp

Abstract

Preparation of sulfide-based Li-ion conductive solid electrolytes by a liquid-phase process has been proposed as an effective route for industrial scaling-up. However, reaction mechanisms in the liquid-phase synthesis or the role of solvents in the reactions are not yet well understood. Here, the reaction between Li_2S and P_2S_5 in the composition of 50:50 mol% mediated by a polar aprotic solvent (acetonitrile) was investigated. The study of the crystal and local structure of the $50Li_2S{:}50P_2S_5$ sample revealed large chemical changes upon crystallization, highlighting the initial formation of a polymer-like $(PS_3^-)_n$ intermediate. In the base of the $(PS_3^-)_n$ intermediate, the reaction pathways for the formation of the $P_2S_6^{2-}$, PS_4^{3-}, and $P_2S_7^{4-}$ anions are elucidated. These findings give a deeper insight into the reaction mechanisms governing the liquid-phase synthesis of sulfide solid electrolytes and provide more specific criteria by which to design novel materials with superior characteristics through this liquid-phase approach.

Introduction

Lithium-ion batteries are proposed as energy storage systems to offer the high energy density required for applications such as the electric vehicle and renewable energy storage [1]. However, conventional Lithium-ion batteries possess safety issues because of the use of flammable organic liquid electrolytes [2, 3]. All-solid-state lithium batteries using inorganic solid electrolytes instead of liquid electrolytes are expected to meet the energy density and safety required [4, 5].

Sulfide-based solid electrolytes are promising solid electrolytes for the application to the all-solid-state battery because they exhibit high ionic conductivity over 10^{-4} S cm^{-1} and have good ductility [6, 7] that facilitates intimate contact with electrode materials. The synthesis of sulfide solid electrolytes often involves a mechanical milling process. Although this technique has been useful for the discovery and design of novel materials [8-10], the size of the mechanical milling jar and the long processing time required (8-50 hours) limit the industrial scaling-up [11].

During the last years, the preparation of sulfide solid electrolytes by a liquid-phase process, using organic solvents to promote the reactions, has been investigated as an alternative to the mechanical milling route [11]. The liquid-phase synthesis is not only a more facile process for the industrial scaling up, it also offers many advantages in relation to the main challenges in the all-solid-state battery. It offers the possibility to form intimate contacts and high surface coverage of solid electrolytes on the electrode materials by their direct precipitation [12, 13], and also it is advantageous for the preparation of thin membranes [14].

In 2013, Liang et al. reported that the magnetic stirring of Li_2S and P_2S_5 in tetrahydrofuran, following by a heat treatment at the relatively low temperature of 140 °C, produced β-Li_3PS_4 with high ionic conductivity of 1.6 x 10^{-4} S cm^{-1} at room temperature [15]. From 2013, several works have reported the successful synthesis of solid electrolytes containing crystal phases such as the β-Li_3PS_4 [13, 16-18], $Li_7P_3S_{11}$ [19-22], and argyrodites [23-25] by using different solvents. Moreover, the $Li_7P_2S_8I$ [26] and Li_4PS_4I [27] crystal phases were discovered by using the liquid-phase approach.

The additional parameters offered by the liquid-phase synthesis, such as the solvent properties (dielectric constant, donor number, chemical structure, etc.), precursors concentrations, as well as temperature and time, gives the possibility of new reaction pathways to find new metastable materials that often exhibit superior properties and that cannot be obtained by high-temperature synthesis, in which the thermodynamically most favored products are usually obtained.

Although great attention has been given to the liquid-phase process of sulfide solid electrolytes during the last years, the reaction mechanisms in the liquid-phase synthesis or the role of solvents in the reactions are not yet well understood [11, 28].

For example, it is known that the specific anion composition and arrangement in the structure of the sulfide solid electrolytes play a key role in their ionic conductivity [29]. In the preparation of Li_2S-P_2S_5 solid electrolytes by mechanical milling, the P_2S_5 precursor suffers an amorphization, and the formation of the different thiophosphate units is controlled by the incorporation of the glass modifier Li_2S [30, 31]. However, the reaction mechanism that takes place in the liquid-phase synthesis that leads to the formation of the different thiophosphate anions is not clear [28].

A better understanding of the mechanism of the reaction for the formation of the different thiophosphate units will provide more specific criteria by which to design the reactions pathways to obtain the desired materials or discover new materials through the liquid-phase synthesis.

In this work, we investigate the reaction between Li_2S and P_2S_5, by the mediation of acetonitrile as an example of polar aprotic solvents, that leads to the formation of the basic thiophosphate anions. Polar aprotic solvents are suitable solvents to avoid decomposition reactions with the precursors.

Experimental section

Synthesis

Li_2S (Mitsuwa Chemical, 99.9%) and P_2S_5 (Aldrich, 99%) were mixed in anhydrous acetonitrile (Wako Pure Chemical Industries, 99.5%). Ultrasonic irradiation for 1 hour at room temperature in an ultrasonic bath (Branson 2200) was applied to enhance the mixing of the precursors.

The obtained solution was subsequently dried at 100 °C or 180 °C for 3 h under vacuum to remove the solvent and obtain solid powders. In addition, the sample dried at 180 °C was heat treated at 220 °C for 1 h.

Solvent evaporation was performed under vacuum. All other processes were performed in an argon atmosphere to avoid hydrolysis of sulfide materials.

Characterization

The crystal phase and local structure of the sample was examined by X-ray diffraction (XRD), Raman spectroscopy and ^{31}P NMR spectroscopy.

XRD measurements were performed using CuKα radiation with an X-ray diffractometer (Miniflex 600, Rigaku). Diffraction data were collected at 0.01° steps from 10° to 40° in 2θ. Raman spectroscopy was performed using a Raman spectrometer (HORIBA XploRA PLUS Scientific) to identify structural units of the samples. Raman shift was ranged between 300 cm^{-1} and 3000 cm^{-1}.

^{31}P MAS NMR (Magic Angle Spinning – Nuclear Magnetic Resonance) spectroscopy was performed using an NMR spectrometer (JEOL JNM-ECZ400R) with rotating speed of 11 kHz. ^{31}P NMR spectroscopy was performed using an NMR spectrometer (JEOL ECX400) at 400 MHz. All processes were performed under argon atmosphere.

Safety considerations

Li_2S caution: Contact with water liberates toxic gas.

P_2S_5 caution: Contact with water liberates toxic gas.

Acetonitrile caution: Acetonitrile is designated as a poisonous substance under Japanese law.

Results and discussion

Figure 1 shows photographs of mixtures of Li_2S and P_2S_5 in stoichiometric compositions of 50:50 mol%, 60:40 mol% and 70:30 mol% in acetonitrile after applying ultrasonic irradiation for 1 h. Li_2S and P_2S_5 in 50:50 mol% resulted in the formation of a clear yellow solution (Figure 1a). Mixtures of Li_2S and P_2S_5 in 60:40 mol% and 70:30 mol% resulted in the formation of whitish suspensions (Figure 1 b and c).

Most of the Li_2S-P_2S_5 solid electrolytes synthesized by liquid-phase containing the β-Li_3PS_4 [16-18] and $Li_7P_3S_{11}$ [19-22] crystal phases have been obtained through the formation of suspensions. However, to the best of our knowledge, there is no report about what chemical species in the Li_2S:P_2S_5 stoichiometric composition of 50:50 mol% with high solubility are readily formed in acetonitrile. Thus, the crystal and local structure of the $50Li_2S$:$50P_2S_5$ sample were investigated by using X-ray diffraction, Raman spectroscopy and ^{31}P NMR spectroscopy.

Figure 2 shows the XRD patterns of the $50Li_2S$:$50P_2S_5$ sample a) after drying at 100 °C, b) after drying at 180 °C and c) after drying at 180 °C and subsequent heat treatment at 220 °C. After drying at 100 °C, the $50Li_2S$:$50P_2S_5$ sample exhibited a halo XRD pattern, and thus it was found to be amorphous. After drying at 180 °C, peaks that are not assigned to known crystals were observed. After heat treatment at 220 °C, peaks corresponding to the $Li_2P_2S_6$ crystal phase were observed.

Figure 3 shows the Raman spectra of the $50Li_2S$:$50P_2S_5$ sample a) after drying at 100 °C, b) after drying at 180 °C and c) after drying at 180 °C and subsequent heat treatment at 220 °C. The Raman spectrum of the sample after drying at 100 °C, exhibited a major band centered at 390 cm^{-1}. Raman bands centered at 235 cm^{-1},

311 cm^{-1}, 500 cm^{-1}, 560 cm^{-1} and 585 cm^{-1} are not attributed to the PS_4^{3-}, $P_2S_7^{4-}$ or $P_2S_6^{4-}$ thiophosphate units, neither to Li_2S or P_2S_5 precursors. The Raman bands centered at 900 cm^{-1}, 1370 cm^{-1}, 2200 cm^{-1} and 2900 cm^{-1} are attributed to the C-C stretch, C-H bend, C≡C stretch and C-H bending vibrations of acetonitrile [32, 33]. The Raman spectrum of the sample obtained after drying at 180 °C, exhibited a similar spectrum to that of the sample obtained after drying at 100 °C, at the lower Raman shift region. At the higher Raman shift region, the Raman bands attributed to acetonitrile were no longer observed. The Raman spectrum of the sample obtained after heat treatment at 220 °C, exhibited mainly two bands centered at 390 cm^{-1} and 417 cm^{-1}, attributed to $P_2S_6^{2-}$ units [34]. The most intense peak at around 417 cm^{-1} has been assigned to the symmetric stretching mode of the P-S-P-S ring in the $P_2S_6^{2-}$ units.

Figure 4 shows the ^{31}P MAS NMR spectra of the $50Li_2S{:}50P_2S_5$ sample a) after drying at 100 °C, b) after drying at 180 °C and c) after drying at 180 °C and subsequent heat treatment at 220 °C. The ^{31}P MAS NMR spectrum of the sample after drying at 100 °C exhibited a signal centered at 85 ppm. The ^{31}P MAS NMR spectrum of the sample after drying at 180 °C, exhibited a signal centered at 83 ppm, attributed to PS_3^- chain units [35]. The ^{31}P MAS NMR spectrum of the sample after heat treatment at 220 °C, exhibited a signal centered at 55 ppm, attributed to $P_2S_6^{2-}$ units [34].

The study of the $50Li_2S{:}50P_2S_5$ sample allowed to clearly identified the formation of the $Li_2P_2S_6$ crystal phase with local structure composed of $P_2S_6^{2-}$ units after the heat treatment at 220 °C. However, the examination of the crystal phase and local structure after each step of the synthesis allowed to detect large chemical changes during the crystallization process. The ^{31}P MAS NMR spectrum of the $50Li_2S{:}50P_2S_5$ sample after drying at 180 °C (Figure 4b) indicated the formation of PS_3^- chain units [35]. The

slightly difference in the chemical shift in the ^{31}P MAS NMR spectrum of the sample after drying at 100 °C (85 ppm) in comparison to the sample obtained after drying at 180 °C (83 ppm) could be ascribed to the presence of remaining acetonitrile molecules in the sample observed by Raman spectroscopy (Figure 3a) that could alter the chemical environment of the PS_3^- chain units. Based on the results from ^{31}P MAS NMR spectroscopy, the major Raman band at 390 cm^{-1}, observed in the Raman spectra of the $50Li_2S{:}50P_2S_5$ sample after drying at 100 °C or 180 °C (Figure 3a and b) is here attributed to PS_3^- chain units. Although, $P_2S_6^{4-}$ units exhibit a Raman band located at the same position [36], the formation of $P_2S_6^{4-}$ units was not observed by ^{31}P MAS NMR spectroscopy. Because the Raman bands centered at 235 cm^{-1}, 311 cm^{-1}, 500 cm^{-1}, 560 cm^{-1}, and 585 cm^{-1} are observed after drying at 100 °C (Figure 3a) but not after the heat treatment at 220 °C (Figure 3c), these bands should relate to a complex containing acetonitrile molecules, that dissociates at high temperature.

The evaluation of the crystal and local structure of the $50Li_2S{:}50P_2S_5$ sample during crystallization allowed to elucidate the formation of PS_3^- chain units prior to the formation of $P_2S_6^{2-}$ units and $Li_2P_2S_6$ crystal phase. This kind of polymeric-like PS_3^- chain units can be expected to exhibit high solubility as shown in Figure 1a.

Figure 5 shows the ^{31}P NMR spectrum of the $50Li_2S{:}50P_2S_5$ solution. The ^{31}P NMR spectrum exhibited chemical shifts at 87.1 (singlet), 85.9 (doublet), 63 (triplet), and 53.7 ppm (doublet), confirming that the P atom is found in different chemical environments as it is expected in the polymer-like PS_3^- chain structure. The J coupling constant of 52 Hz was calculated for doublet and triplet signals, and it is assigned to the P-P coupling through the P-S-P bonds in the PS_3^- chains. The major signal at 87.1 ppm can be assigned to the P atom in the end of group of the PS_3^- chain units,

because a similar chemical environment to that of the P atom in the PS_4^{3-} units, that exhibit a ^{31}P NMR signal at 89-87 ppm [34], is expected.

The ratio of the ^{31}P NMR signal attributed to the end of group of the PS_3^- chain units (87.1 ppm) to the ^{31}P NMR signal at 85.9 ppm was 1 to 0.31. However, it was 1 to 0.45 in a $50Li_2S{:}50P_2S_5$ solution that was stored for one day. It suggests that a polymerization reaction proceeds with time. This polymerization reaction can be expected to also proceed with temperature, which could also contribute to the slight shift in the ^{31}P NMR signal with the increase in the temperature (Figure 4 a and b).

The proposed reaction pathway for the formation of the meta-thiodiphosphate $P_2S_6^{2-}$ anion through the liquid-phase process is illustrated in Scheme 1. It is generally accepted that the precursor phosphorus pentasulfide, the P_4S_{10} molecule, can dissociate into the reactive P_2S_5 under the refluxing of solvents such as acetonitrile [37]. The P_2S_5 molecule is in an unfavorable $\sigma^3\lambda^5$ bonding situation and is unstable unless the missing forth coordination partner for the phosphorus atom is provided [38]. This strong Lewis acidity in P_2S_5 is believed to be the reason for the rapid reaction with Li_2S to form high-soluble polymer-like PS_3^- chains. The PS_3^- chain units were found to be stable at or below 180 °C; however, at temperatures above 220 °C, the PS_3^- chain units converted to the meta-thiodiphosphate $P_2S_6^{2-}$ units.

Although the reaction between Li_2S and P_2S_5 in acetonitrile readily proceed to the formation of PS_3^- chains, the $P_2S_6^{2-}$ units that are formed upon heat treatment, are not favorable for the Li^+ conduction (2.5×10^{-9} S cm^{-1} at room temperature, Figure S1). Higher ionic conductivity has been found in Li_2S-P_2S_5 solid electrolytes with higher Li_2S content than 50 mol%, achieving ionic conductivities over 10^{-3} S cm^{-1} attributed to the formation of PS_4^{3-} and $P_2S_7^{4-}$ units that favor the Li^+ conduction [30, 31].

We have previously reported the possible formation of PS_4^{3-} units from Li_2S and P_2S_5 in compositions with Li_2S content between 70 and 75 mol% by the mediation of acetonitrile [17, 19]. Scheme 2 illustrates the proposed reaction pathway for the formation of the orthothiophosphate PS_4^{3-} anion through liquid-phase using acetonitrile as the medium for the reaction. Formally, PS_4^{3-} units are formed from the stoichiometric composition $3Li_2S{:}1P_2S_5$ ($75Li_2S{:}25P_2S_5$ mol%), with an excess of Li_2S in comparison to the composition with the 1:1 molar ratio ($50Li_2S{:}50P_2S_5$ mol%). It can be expected that in the first step of the reaction, Li_2S and P_2S_5 in 1:1 molar ratio react to form the PS_3^- chains, and that in a second step of the reaction, the additional Li_2S be incorporated as terminal sulfur with Li^+ acting as the counterion, resulting in the breaking of the P-S-P bridges in the PS_3^- chains and therefore in the formation of isolated PS_4^{3-} units with negligible solubility in acetonitrile and exhibiting white color [19].

A similar mechanism of reaction can be expected for the formation of $P_2S_7^{4-}$ units. However, as reported elsewhere [19], the formation of $P_2S_7^{4-}$ units has been observed only after heat treatment at temperatures above 180 °C [19], indicating that the $P_2S_7^{4-}$ units could not be stable in the solution or suspension state. Scheme 3 illustrates the proposed reaction pathway for the formation of the pyrothiophosphate $P_2S_7^{4-}$ anion through the liquid-phase process using acetonitrile as the medium for the reaction. As described above, PS_3^- chains would be rapidly formed in the stoichiometric composition of Li_2S and P_2S_5 of 50:50 mol%, the further incorporation of Li_2S would break the P-S-P bridges in the PS_3^- chains resulting in the formation of isolated PS_4^{3-} units. However, for a total Li_2S content less than 75 mol%, the sulfur provided by the Li_2S is not enough to break all the P-S-P bridges in the PS_3^- chains. Therefore, for a certain step of the reaction PS_4^{3-} units would coexist with remaining PS_3^- chains. After

complete solvent removal and upon heat treatment at temperature above 180 °C, the PS_4^{3-} and PS_3^- chains units would react to form the $P_2S_7^{4-}$ units.

The proposed reaction mechanism for the formation of $P_2S_7^{4-}$ units in this work is in good agreement with the findings of Wang et al. [39]. It was reported that after mixing for three days a mixture of Li_2S and P_2S_5 with stoichiometric composition of 70:30 mol% in acetonitrile, if the precipitated phase is separated from the supernatant, after heat treatment at 260 °C, the precipitated phase exhibited only the formation of PS_4^{3-} units, and the supernatant exhibited the formation of $P_2S_6^{2-}$ and $P_2S_6^{4-}$ units. No formation of $P_2S_7^{4-}$ units was found in the precipitated phase neither in the supernatant. However, the formation of $P_2S_7^{4-}$ units was clearly observed after heat treatment at 260 °C, when the separation of phases was not carried out [39].

The reaction between the PS_4^{3-} units and the PS_3^- chains units to form the $P_2S_7^{4-}$ units is here associated with redox processes that could take place upon heat treatment. It can be expected that the PS_3^- chains proceed to the formation of the corner-sharing $P_2S_7^{4-}$ units (Eq. (2)), by an S^{2-} transfer from the PS_4^{3-} units (Eq. (1)). This kind of redox processes in the PS_4^{3-} units have been observed before [40].

$$2\ PS_4^{3-} + 6\ Li^+ \longrightarrow P_2S_7^{4-} + 4Li^+ + S^{2-} + 2Li^+ \quad (1)$$

$$(PS_3^-)_2 + 2Li^+ + S^{2-} + 2\ Li^+ \longrightarrow P_2S_7^{4-} + 4Li^+ \quad (2)$$

Although acetonitrile was used as the solvent in this work, a similar mechanism of reaction can be expected in other polar aprotic solvents such as ethyl propionate[41], dimethoxyethane [20] and tetrahydrofuran [22].

Conclusions

The mechanism of formation of the basic thiophosphate anions through the liquid-phase synthesis, using acetonitrile as the medium, was elucidated. The dissociation of the P_4S_{10} molecule into the reactive P_2S_5 is expected to favor a rapid reaction with Li_2S to form polymer-like PS_3^- chains exhibiting high solubility. The PS_3^- chains react upon heat treatment at temperatures above 180 °C to form $P_2S_6^{2-}$ units, as it was confirmed by Raman and ^{31}P MAS NMR spectroscopies. It is proposed that the formation of the PS_3^- chain units also constitute the initial step of the reaction for the formation of the PS_4^{3-} and $P_2S_7^{4-}$ anions. In compositions with Li_2S content higher than 50 mol%, the increase in the sulfur content is believed to break the P-S-P bridges in the PS_3^- chains, resulting in the formation of isolated PS_4^{3-} units. If sulfur provided by Li_2S is not enough to break all P-S-P bridges, it is hypothesized that the PS_4^{3-} units and the remaining PS_3^- chains undergo redox processes upon heat treatment (>180 °C) that results in the formation of the $P_2S_7^{4-}$ units.

Acknowledgements

The present work was partially supported by the Japan Science and Technology Agency (JST), the Advanced Low Carbon Technology Research and Development Program (ALCA), and the Specially Promoted Research for Innovative Next Generation Batteries (SPRING) project.

Supporting Information

Arrhenius plot of the $50Li_2S{:}50P_2S_5$ sample after drying at 100 °C, after drying at 180 °C, and after drying at 180 °C and subsequent heat treatment at 220 °C.

References

[1] J.-M. Tarascon, M. Armand, Issues and challenges facing rechargeable lithium batteries, Materials for Sustainable Energy: A Collection of Peer-Reviewed Research and Review Articles from Nature Publishing Group, World Scientific2011, pp. 171-179.

[2] M. Armand, J.-M. Tarascon, Building better batteries, nature, 451 (2008) 652.

[3] J.B. Goodenough, Y. Kim, Challenges for rechargeable Li batteries, Chem. Mater., 22 (2009) 587-603.

[4] K. Takada, Progress and prospective of solid-state lithium batteries, Acta Mater., 61 (2013) 759-770.

[5] A. Hayashi, A. Sakuda, M. Tatsumisago, Development of sulfide solid electrolytes and interface formation processes for bulk-type all-solid-state Li and Na batteries, Frontiers in Energy Research, 4 (2016) 25.

[6] A. Kato, M. Nose, M. Yamamoto, A. Sakuda, A. Hayashi, M. Tatsumisago, Mechanical properties of sulfide glasses in all-solid-state batteries, J. Ceram. Soc. Jpn., 126 (2018) 719-727.

[7] A. Sakuda, A. Hayashi, M. Tatsumisago, Sulfide Solid Electrolyte with Favorable Mechanical Property for All-Solid-State Lithium Battery, Sci Rep, 3 (2013) 1-5.

[8] Y. Seino, T. Ota, K. Takada, A. Hayashi, M. Tatsumisago, A sulphide lithium super ion conductor is superior to liquid ion conductors for use in rechargeable batteries, Energ Environ Sci, 7 (2014) 627-631.

[9] N. Kamaya, K. Homma, Y. Yamakawa, M. Hirayama, R. Kanno, M. Yonemura, T. Kamiyama, Y. Kato, S. Hama, K. Kawamoto, A. Mitsui, A lithium superionic conductor, Nat. Mater., 10 (2011) 682-686.

[10] Y. Kato, S. Hori, T. Saito, K. Suzuki, M. Hirayama, A. Mitsui, M. Yonemura, H. Iba, R. Kanno, High-power all-solid-state batteries using sulfide superionic conductors, Nat. Energy, 1 (2016) 7.

[11] A. Miura, N.C. Rosero-Navarro, A. Sakuda, K. Tadanaga, N.H. Phuc, A. Matsuda, N. Machida, A. Hayashi, M. Tatsumisago, Liquid-phase syntheses of sulfide electrolytes for all-solid-state lithium battery, Nature Reviews Chemistry, 3 (2019) 189-198.

[12] S. Chida, A. Miura, N.C. Rosero-Navarro, M. Higuchi, N.H. Phuc, H. Muto, A. Matsuda, K. Tadanaga, Liquid-phase synthesis of Li_6PS_5Br using ultrasonication and application to cathode composite electrodes in all-solid-state batteries, Ceram. Int., 44 (2018) 742-746.

[13] S. Teragawa, K. Aso, K. Tadanaga, A. Hayashi, M. Tatsumisago, Liquid-phase synthesis of a Li_3PS_4 solid electrolyte using *N*-methylformamide for all-solid-state lithium batteries, J. Mater. Chem. A, 2 (2014) 5095-5099.

[14] Z.D. Hood, H. Wang, A.S. Pandian, R. Peng, K.D. Gilroy, M. Chi, C. Liang, Y. Xia, Fabrication of Sub-Micrometer-Thick Solid Electrolyte Membranes of β-Li_3PS_4 via Tiled Assembly of Nanoscale, Plate-Like Building Blocks, Adv. Energy Mater, 8 (2018) 1800014.

[15] Z.C. Liu, W.J. Fu, E.A. Payzant, X. Yu, Z.L. Wu, N.J. Dudney, J. Kiggans, K.L. Hong, A.J. Rondinone, C.D. Liang, Anomalous High Ionic Conductivity of Nanoporous β-Li_3PS_4, J. Am. Chem. Soc., 135 (2013) 975-978.

[16] N.H.H. Phuc, M. Totani, K. Morikawa, H. Muto, A. Matsuda, Preparation of Li_3PS_4 solid electrolyte using ethyl acetate as synthetic medium, Solid State Ionics, 288 (2016) 240-243.

[17] H. Wang, Z.D. Hood, Y.N. Xia, C.D. Liang, Fabrication of ultrathin solid electrolyte membranes of β-Li_3PS_4 nanoflakes by evaporation-induced self-assembly for all-solid-state batteries, J. Mater. Chem. A, 4 (2016) 8091-8096.

[18] N.H.H. Phuc, K. Morikawa, T. Mitsuhiro, H. Muto, A. Matsuda, Synthesis of plate-like Li_3PS_4 solid electrolyte via liquid-phase shaking for all-solid-state lithium batteries, Ionics, 23 (2017) 2061-2067.

[19] M. Calpa, N.C. Rosero-Navarro, A. Miura, K. Tadanaga, Instantaneous preparation of high lithium-ion conducting sulfide solid electrolyte $Li_7P_3S_{11}$ by a liquid phase process, RSC Adv., 7 (2017) 46499-46504.

[20] S. Ito, M. Nakakita, Y. Aihara, T. Uehara, N. Machida, A synthesis of crystalline $Li_7P_3S_{11}$ solid electrolyte from 1, 2-dimethoxyethane solvent, J. Power Sources, 271 (2014) 342-345.

[21] X.Y. Yao, D. Liu, C.S. Wang, P. Long, G. Peng, Y.S. Hu, H. Li, L.Q. Chen, X.X. Xu, High-Energy All-Solid-State Lithium Batteries with Ultralong Cycle Life, Nano Lett., 16 (2016) 7148-7154.

[22] R.C. Xu, X.H. Xia, Z.J. Yao, X.L. Wang, C.D. Gu, J.P. Tu, Preparation of $Li_7P_3S_{11}$ glass-ceramic electrolyte by dissolution-evaporation method for all-solid-state lithium ion batteries, Electrochim. Acta, 219 (2016) 235-240.

[23] S. Yubuchi, M. Uematsu, C. Hotehama, A. Sakuda, A. Hayashi, M. Tatsumisago, An argyrodite sulfide- based superionic conductor synthesized by a liquid- phase technique with tetrahydrofuran and ethanol, J. Mater. Chem. A, 7 (2019) 558-566.

[24] S. Yubuchi, H. Tsukasaki, A. Sakuda, S. Mori, A. Hayashi, M. Tatsumisago, Quantitative analysis of crystallinity in an argyrodite sulfide-based solid electrolyte synthesized via solution processing, RSC Adv., 9 (2019) 14465-14471.

[25] D.A. Ziolkowska, W. Arnold, T. Druffel, M. Sunkara, H. Wang, Rapid and economic synthesis of a Li_7PS_6 solid electrolyte from a liquid approach, ACS Appl. Mater. Interfaces, 11 (2019) 6015-6021.

[26] E. Rangasamy, Z. Liu, M. Gobet, K. Pilar, G. Sahu, W. Zhou, H. Wu, S. Greenbaum, C. Liang, An iodide-based $Li_7P_2S_8I$ superionic conductor, J. Am. Chem. Soc., 137 (2015) 1384-1387.

[27] S.J. Sedlmaier, S. Indris, C. Dietrich, M. Yavuz, C. Dräger, F. von Seggern, H. Sommer, J.r. Janek, Li_4PS_4I: a Li^+ superionic conductor synthesized by a solvent-based soft chemistry approach, Chem. Mater., 29 (2017) 1830-1835.

[28] M. Ghidiu, J. Ruhl, S.P. Culver, W.G. Zeier, Solution-based synthesis of lithium thiophosphate superionic conductors for solid-state batteries: a chemistry perspective, J. Mater. Chem. A, 7 (2019) 17735-17753.

[29] Y. Wang, W.D. Richards, S.P. Ong, L.J. Miara, J.C. Kim, Y. Mo, G. Ceder, Design principles for solid-state lithium superionic conductors, Nat. Mater., 14 (2015) 1026-1031.

[30] F. Mizuno, A. Hayashi, K. Tadanaga, M. Tatsumisago, High lithium ion conducting glass-ceramics in the system Li_2S-P_2S_5, Solid State Ionics, 177 (2006) 2721-2725.

[31] C. Dietrich, D.A. Weber, S.J. Sedlmaier, S. Indris, S.P. Culver, D. Walter, J. Janek, W.G. Zeier, Lithium ion conductivity in Li_2S-P_2S_5 glasses - building units and local structure evolution during the crystallization of superionic conductors Li_3PS_4, $Li_7P_3S_{11}$ and Li_4P2S_7, J. Mater. Chem. A, 5 (2017) 18111-18119.

[32] C. Chen, X. Huang, D. Lu, Y. Huang, B. Han, Q. Zhou, F. Li, T. Cui, High pressure Raman spectroscopy investigation on acetonitrile and acetonitrile-water mixture, RSC Adv., 5 (2015) 84216-84222.

[33] J.C. Deàk, L.K. Iwaki, D.D. Dlott, Vibrational Energy Redistribution in Polyatomic Liquids: Ultrafast IR−Raman Spectroscopy of Acetonitrile, J. Phys. Chem. A, 102 (1998) 8193-8201.

[34] C. Dietrich, D.A. Weber, S. Culver, A. Senyshyn, S.J. Sedlmaier, S. Indris, J.r. Janek, W.G. Zeier, Synthesis, structural characterization, and lithium ion conductivity of the lithium thiophosphate $Li_2P_2S_6$, Inorg. Chem., 56 (2017) 6681-6687.

[35] H. Eckert, Z. Zhang, J.H. Kennedy, Structural transformation of non-oxide chalcogenide glasses. The short-range order of lithium sulfide (Li_2S)-phosphorus pentasulfide (P_2S_5) glasses studied by quantitative phosphorus-31, lithium-6, and lithium-7 high-resolution solid-state NMR, Chem. Mater., 2 (1990) 273-279.

[36] K. Ohara, A. Mitsui, M. Mori, Y. Onodera, S. Shiotani, Y. Koyama, Y. Orikasa, M. Murakami, K. Shimoda, K. Mori, Structural and electronic features of binary Li_2S-P_2S_5 glasses, Sci Rep, 6 (2016) 1-9.

[37] T. Ozturk, E. Ertas, O. Mert, A berzelius reagent, phosphorus decasulfide (P_4S_{10}), in organic syntheses, Chem. Rev., 110 (2010) 3419-3478.

[38] S. Schönberger, C. Jagdhuber, L. Ascherl, C. Evangelisti, T.M. Klapötke, K. Karaghiosoff, New Acyclic Neutral Phosphorus Sulfides and Sulfide Oxides, Z. Anorg. Allg. Chem., 640 (2014) 68-75.

[39] Y. Wang, D. Lu, M. Bowden, P.Z. El Khoury, K.S. Han, Z.D. Deng, J. Xiao, J.-G. Zhang, J. Liu, Mechanism of formation of $Li_7P_3S_{11}$ solid electrolytes through liquid phase synthesis, Chem. Mater., 30 (2018) 990-997.

[40] R. Koerver, F. Walther, I. Aygün, J. Sann, C. Dietrich, W.G. Zeier, J. Janek, Redox-active cathode interphases in solid-state batteries, J. Mater. Chem. A, 5 (2017) 22750-22760.

[41] R. Matsuda, E. Hirahara, N.H.H. Phuc, H. Muto, H. Tsukasaki, S. Mori, A. Matsuda, Preparation of $LiNi_{1/3}Mn_{1/3}Co_{1/3}O_2/Li_3PS_4$ cathode composite particles using a new liquid-phase process and application to all-solid-state lithium batteries, J. Ceram. Soc. Jpn., 126 (2018) 826-831.

Figures

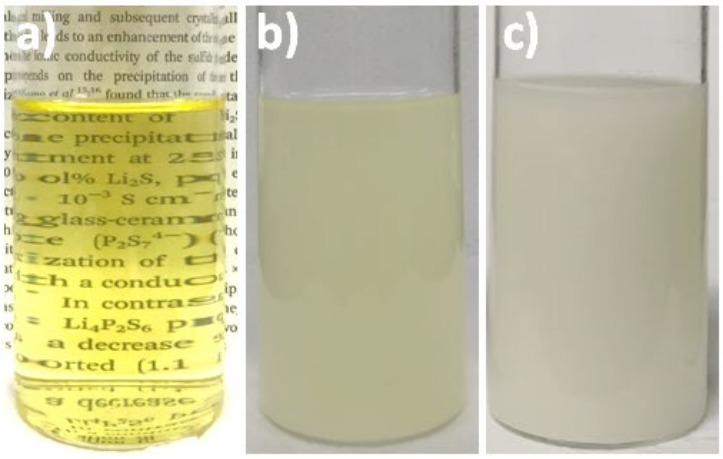

Figure 1. Photographs of mixtures of Li_2S and P_2S_5 in acetonitrile, in the Li_2S:P_2S_5 stoichiometric compositions of **a)** 50:50, **b)** 60:40 and **c)** 70:30 in mol%.

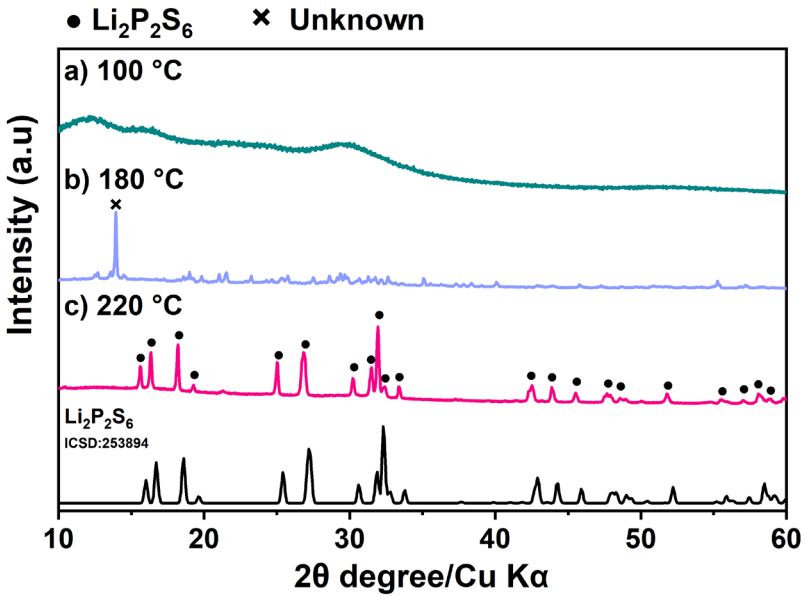

Figure 2. XRD patterns of the $50Li_2S{:}50P_2S_5$ sample **a)** after drying at 100 °C, **b)** after drying at 180 °C and **c)** after drying at 180 °C and subsequent heat treatment at 220 °C. Indexed diffraction pattern of the $Li_2P_2S_6$ crystal phase (ICSD:253894) is shown for comparison.

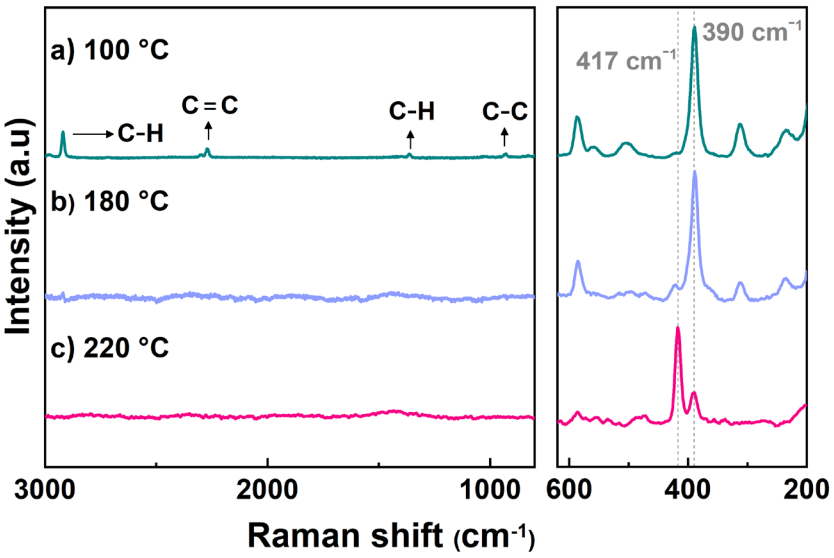

Figure 3 Raman spectra of the $50Li_2S:50P_2S_5$ sample **a)** after drying at 100 °C, **b)** after drying at 180 °C and **c)** after drying at 180 °C and subsequent heat treatment at 220 °C.

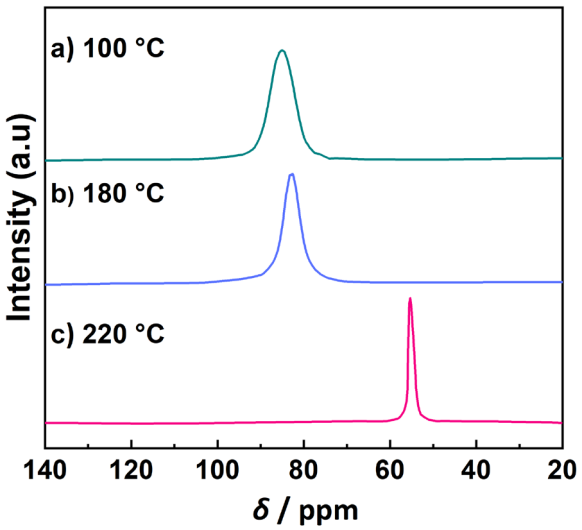

Figure 4. ^{31}P MAS NMR spectra of the $50Li_2S:50P_2S_5$ sample **a)** after drying at 100 °C, **b)** after drying at 180 °C and **c)** after drying at 180 °C and subsequent heat treatment at 220 °C

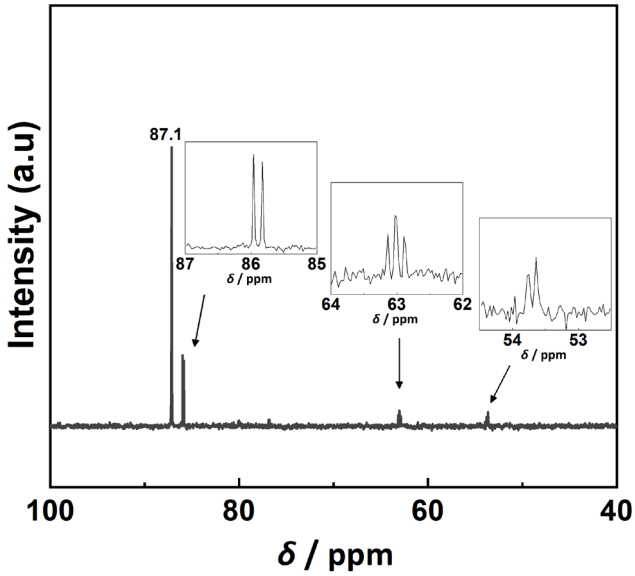

Figure 5. ^{31}P NMR spectrum of the $50Li_2S{:}50P_2S_5$ solution.

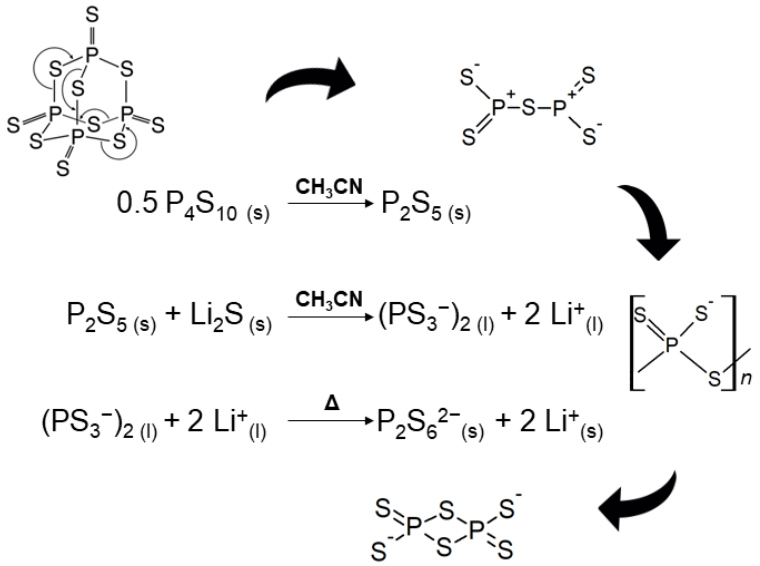

Scheme 1. Reaction pathway for the formation of the meta-thiodiphosphate $P_2S_6^{2-}$ anion.

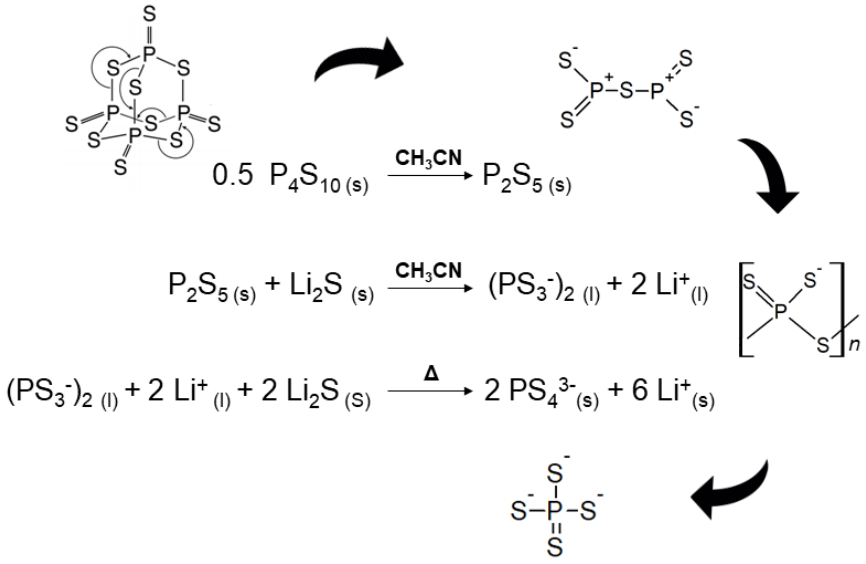

Scheme 2. Reaction pathway for the formation of the orthothiophosphate PS_4^{3-} anion.

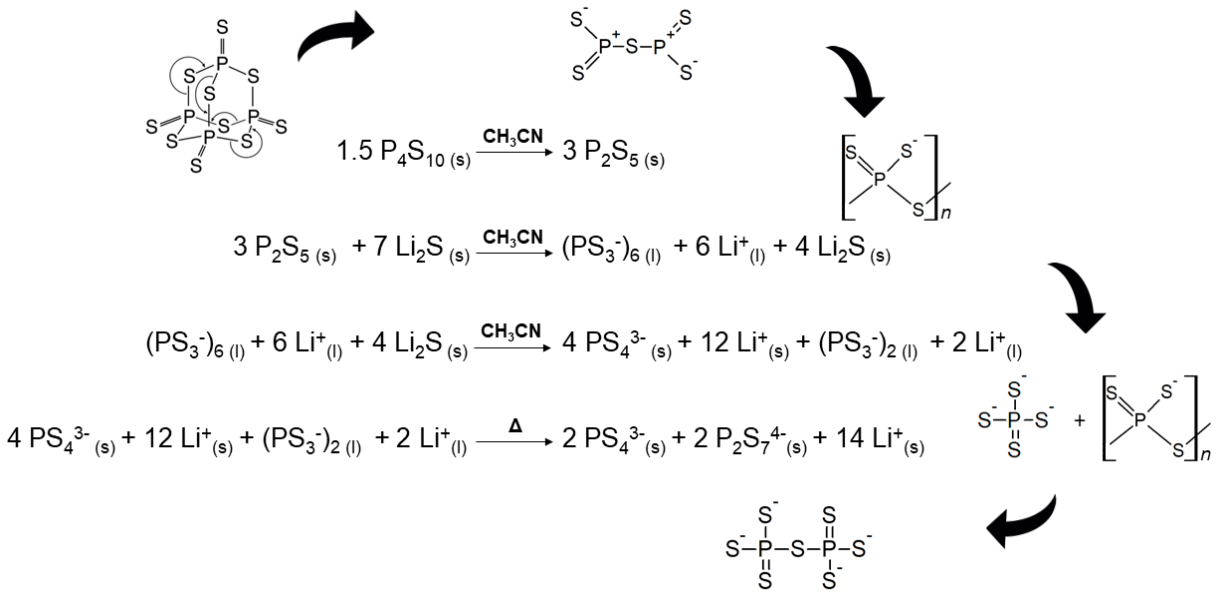

Scheme 3. Reaction pathway for the formation of the pyrothiophosphate $P_2S_7^{4-}$ anion.

Abstract Graphic